İSTANBUL UNIVERSITY CERRAHPAŞA

**RESEARCH ARTICLE**

Electrica 2021; 21(2): 235-241

# Analysis and Design of a Flyback Converter for Universal Input and Wide Load Ranges

**Ferudun Gökçegöz, Erdem Akboy, A. Hülya Obdan**

Department of Electric and Electronic Faculty, Electrical Engineering, Yıldız Technical University, İstanbul, Turkey

**Cite this article as:** F. Gökçegöz, E. Akboy, A. H. Obdan, "Analysis and Design of a Flyback Converter for Universal Input and Wide Load Ranges", Electrica, vol. 21, no. 2, pp. 235-241, May, 2021.

**ABSTRACT**

Flyback converters exhibit the advantages of simple structure, low cost, small volume, isolation, and control simplicity. However, flyback converters demonstrate disadvantages like leakage inductance; hence, losses are incurred. Losses pertain to the requirement of an external cooling system and external costs. It also results in low efficiency and the use of flyback converters in low-power applications. The discontinuous conduction mode (DCM) is used for low-power applications to achieve efficiency. In flyback converters, the reverse recovery losses of the diode are eliminated with DCM. There are many applications of flyback converters in industrial systems, such as led drivers, battery charge systems, telecommunication systems. In this study, analysis and design of a flyback converter for universal input and wide load ranges was performed. The detailed theoretical analysis was conducted and verified with the implementation of a DCM flyback converter for 85 V-265 V RMS AC input voltage, 12 Vo output, 100 kHz switching frequency, and 48 W output power. The overall efficiency of the proposed converter at full load was measured as 81%. Additionally, external cooling systems were not required, which highlighted the development of a compact design with small volume and ease of application for an industrial system that requires the inclusion of more serial flyback converters.

**Keywords:** DC-DC converter, flyback converter, wide load range

**Corresponding Author:**
Erdem Akboy

**E-mail:**
eakboy@yildiz.edu.tr

**Received:** November 11, 2020

**Accepted:** December 17, 2020

**Available Online Date:**
May 20, 2021

**DOI:** 10.5152/electrica.2021.20092



## Introduction

The use of energy with high efficient and quality is of importance depending on the welfare level of societies and technological developments. Additionally, energy consumption continues to increase, and energy renewal has emerged as a global issue. Pulse Width Modulated (PWM) DC-DC converters are widely used in industry owing to properties, such as fast dynamic response, ease of control, and simplicity of structure. They are divided into two types, namely isolated and non-isolated DC-DC converters [1-15].

Non-isolated DC-DC converters are categorized as buck, boost, and buck-boost converters. These converters are used in several industrial systems. Although they possess a simple structure, they are not safe for electrical applications since there is no isolation between input and output. Isolated DC-DC converters, such as flyback and forward converters, are used in several industrial applications. Forward converters possess additional winding to reset magnetizing energy. In the volumes of these converters are greater than those of flyback converters [6-10].

There are two modes for resetting the magnetizing inductance current within a switching period. Inthe Continuous Current Mode (CCM), the magnetizing current does not decrease to a value of zero. There is continuous processing of energy from input to output. Hence, they are used in high-power applications. In the Discrete Current Mode (DCM), the magnetizing current decrease to a value of zero and remains at zero among the switching cycle. In this mode, current peaks of the power components are higher than those observed in the CCM mode operation. However, reverse recovery losses of diodes are eliminated, and Soft Switching (SS) is also provided. Thus, the efficiency of the DCM operation is higher than the CCM ones [11-15].

The primary-side-regulation (PSR) flyback converter is being increasingly adopted in general lighting applications, owing to its elimination of the opto-coupler, simple control mode, good electrical isolation, high efficiency, compact size, and low cost [8].

In this study, analysis and design of a flyback converter for universal input and wide output ranges have been discussed. In this study, to verify the theoretical analysis, the detailed theoretical analysis was confirmed by an application circuit with input voltage of 85-265 VAC, output voltage of 12 VDC, output power of 12 W-48 W, and a switching frequency of 100 kHz. The total efficiency of the converter increased to 81%. Furthermore, an external cooling system was not necessary, which eliminated the obtainment of high-volume converters owing to the design parameters. Therefore, it is not suitable for the applications where they require many flyback converters.

## Theoretical Method

### Definitions and assumptions

The designed circuit diagram of the flyback converter with control scheme is depicted in Figure 1. This converter was designed using input filter component, rectifier bridge, rectifier filter capacitor $C_i$, transformer TR, MOSFET M, Schottky diode D, and output capacitor $C_o$. At this converter input, the AC voltage and the load are variable. Furthermore, MOSFET is selected since they are suitable for low-power and high-frequency applications.

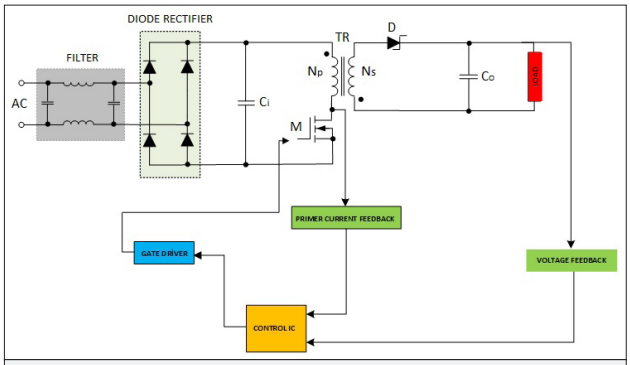


**Figure 1.** The conventional flyback converter circuit scheme with control units

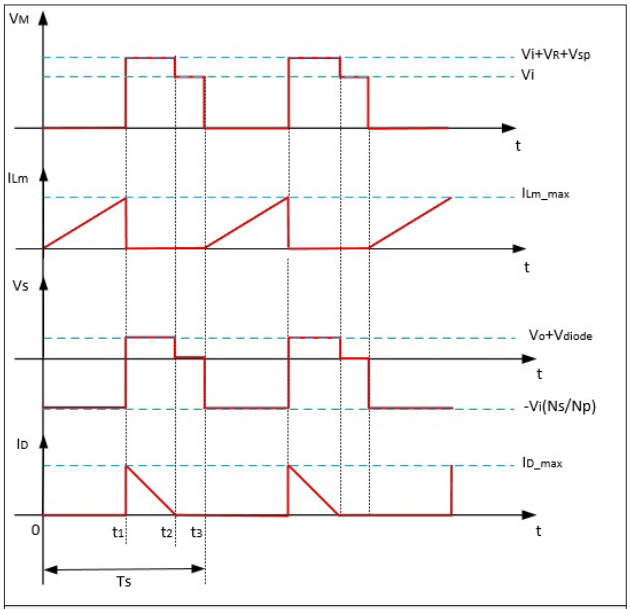


**Figure 2.** The key waveforms of the conventional flyback converter

The following assumptions have been considered to facilitate steady-state analysis during a switching period.

- The rectified input voltage $V_i$ is constant.
- The output capacitor $C_o$ is substantial enough to accept the output voltage $V_o$ constant.
- The leakage inductance is negligible for the stages.
- All semiconductors are ideal.

### Operation Stages

In the designed flyback, three different intervals occur during one switching period $T_s$. The key waveforms for the stages are presented in Figure 2.

### Initial status

During this interval, the load is provided from only the output capacitor and magnetizing inductance has been reset.

#### *Stage 1 ($t_0$<t<$t_1$)*

This stage begins when the control signal is applied to the gate-source terminal of the MOSFET. In this interval, transformer magnetizing inductance current increases linearly from zero via the rectified and filtered input voltage. The following equations are valid for this interval.

$$i_{Lm} = \frac{V_i}{L_m} t \quad (1)$$

where $L_m$ represents the magnetizing inductance, and $i_{Lm}$ represents the magnetizing current. This interval ends with disruption of the control signal of M.

#### Stage 2 *($t_1$<t<$t_2$)*

At the beginning of this stage, $i_M = 0$ and $i_D = I_{D\_max}$. After the M signal is turned off, D is turned on and this stage begins. At this stage, magnetizing energy is transferred to the output. For this interval,

$$i_D = I_{D\_max} - \frac{V_o}{L_s} t \quad (2)$$

$$I_{D\_max} = I_{M\_max} n \quad (3)$$

are valid. In these equations, $L_S$ represents the seconder windings of TR, $I_{D—max}$ represents the maximum current of the diode, and n represents the turn ratio of the transformer primary and seconder windings. This interval ends when the diode current reaches a value of zero. Hence, reverse recovery losses are eliminated.

#### *Stage 3 ($t_2$<t<$t_3$)*

This interval begins when the diode current reaches a value of zero. In this interval, magnetizing inductance energy is zero, and the output is provided from the output capacitor. This stage ends when the control signal is applied to M.

### Design Procedure

The selection criteria of the proposed wide input-wide output range flyback are prescribed according to the 85 V-265 V

RMS input voltage and 12 V DC output voltage with 100 kHz switching frequency. The output power varies for 20% and 100% load.

**Input Analysis**

The input power is calculated assuming the maximum efficiency is 80%.

$$P_i = \frac{P_o}{\eta} \quad (4)$$

In this equation, η represents the efficiency term. For the aforementioned values, the input power is calculated as 60 W. The input capacitor is determined as listed in Table 1, with the expression of μF/W considered as per the values reported in literature and based on experience.

After the capacitor value is determined, the ripple amount is calculated according to the following equation and the Figure 3.

$$V_{i\_min} = \sqrt{2V_{AC}^2 - \frac{P_i(1-RF)}{C_i f_{AC}}} \quad (5)$$

$$V_{i\_max} = \sqrt{2}V_{AC\_max} \quad (6)$$

$$\Delta V_i = V_{i\_max} - V_{i\_min} \quad (7)$$

In these equations, $f_{AC}$ represents the line frequency, and RF represents ripple factor. RF is selected as 0.2 and $V_{i—max}$ is 375 V for 265 VAC input voltage, and $V_{i\_}$ min is 90 V.

$t_c$ represents the capacitor charge time in this Figure3. The rectifier diodes can be selected according to the following criterion for power factor (PF). It is calculated as 1.41 A.

$$I_{Di\_RMS} = \frac{P_i}{PFV_{AC\_min}} \quad (8)$$

**Table 1.** Parameters of the input capacitor

| Input Voltage Range | Capacitor |
|---|---|
| 85 V – 265 V | 2 – 3 μF /W |
| 195 V – 265 V | 1 μF /W |
| 115 V | 2 μF /W |
| 230 V | 1 μF /W |

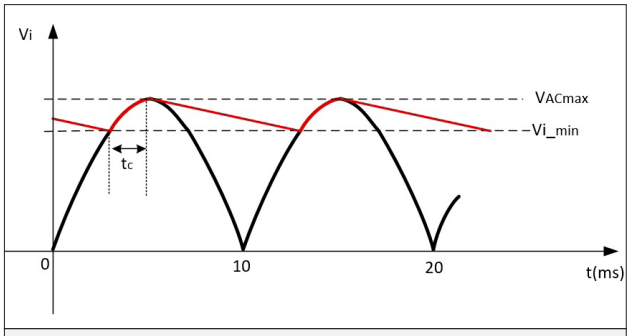


**Figure 3.** The voltage waveform of the rectifier capacitor

**Maximum Voltage Stress and Maximum Duty Cycle Analysis**

While MOSFET is in a turned off condition, the voltage on it is equal to the sum of the DC input voltage and the reflected voltage $V_R$, which is related to the turn ratio of the transformer. Additionally, values for voltage spikes $V_{sp}$ that occur due to leakage inductance during the turn off interval can also be added. $V_R$ can be selected as 75 V in the universal input voltage.

$$V_{M\_max} = V_{AC\_max} + V_R + V_{sp} \quad (9)$$

Maximum duty cycle can be determined using the following equation.

$$D_{max} = \frac{V_R}{V_R + V_{i\_min}} \quad (10)$$

The maximum duty cycle is calculated as 0.46.

**Transformer Analysis**

The turn ratio is calculated based on the $V_R$ value. Selection of an extremely high value will cause a high conversion rate; hence, it will cause more voltage stresses on the MOSFET and less voltage stress on the output diode. Selection of an extremely low value will result in a low conversion rate, which will lead to the occurrence of an opposite trend. Therefore, an optimum value should be selected as the formula mentioned below, wherein, $V_{diode}$ Selection of an extremely high value the forward voltage of the diode when it is in the on-state.

$$n = \frac{V_R}{V_o + V_{diode}} \quad (11)$$

Assuming $V_{diode}$ is 0.5, n can be calculated as 6.

The inductance value to be calculated is the maximum value of the primary magnetizing inductance of the flyback transformer. Since this inductance value is calculated according to the maximum load condition, it is regarded as the critical inductance value for the system's operating mode to switch from DCM to CCM.

$$L_{P\_max} = \frac{(V_{i\_min}D_{max})^2}{2P_i f_s} \quad (12)$$

So, $L_{P\_max}$ is calculated as 143 μH. The number of turns can be calculated for the selected E type cores. We selected E30 type core, whose $A_e$ was 60 mm$^2$. Furthermore, the B magnetic flux density is 0.3-0.4 for 100-kHz applications. Additionally, $A_e$ is the cross-sectional area of the core. thus, the primary number of turns ($N_p$) can be calculated as 36 according to the following formula.

$$N_{P\_min} = \frac{L_m I_{m\_max}}{BA_e} \quad (13)$$

$N_S$ represents secondary number of turns and is calculated according to (11) and (13) as 6.

**Output Capacitor Analysis**

The output capacitor is selected for calculation based on the below-mentioned formula. In this equation, $V_{o\_ripple}$ represents a value that is 1% of the average output voltage.

$$C_o = \frac{I_o.N}{f_s V_{o\_ripple}} \quad (14)$$

**Experimental Results**

Theoretical analysis is confirmed by using an application circuit with 85 V-265 V AC input voltage, 12 VDC output voltage, 48 W output power, and 100 kHz switching frequency. Parameters of the implementation circuit are listed in Table 2.

In Figure 4, the current waveform of the switch according to the control signal and diode voltage is provided for 220 V AC with full load. It can be inferred that DCM is achieved perfectly.

**Table 2.** Parameters of the implementation circuit

| Parameter | Symbol | Values | Model |
|---|---|---|---|
| Input Voltage | $V_{AC}$ | 85 V-265 V | - |
| Output Voltage | $V_o$ | 12 V | - |
| Output Power | $P_o$ | 48 W | - |
| Switching Frequency | $f_s$ | 100 kHz | - |
| Filter Capacitor | $C_i$ | 150 µF | Elektrolytic |
| Output Capacitor | $C_o$ | 333 µF | Elektrolytic |
| Primer Inductance | $L_p$ | 140 µH | E30 core |
| Seconder Inductance | $L_s$ | 3.8 µH | Np=36 Ns=6 |

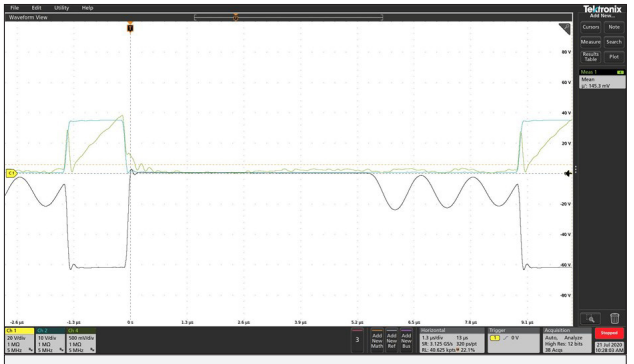

**Figure 4.** The current waveform of the switch with diode voltage according to the control signal

**Figure 5.** The voltage stresses of the MOSFET for 85 V RMS

In Figure 5 and Figure 6, the voltage stresses of the switch are provided for 85 V and 265 V, respectively. The voltage stresses of the MOSFET cannot exceed 400 V at the worst conditions with the appropriate snubber circuit. The photograph of the prototype is presented in Figure 7. It can be inferred that the volume of the circuit is extremely small.

The thermal measurements of the prototype of the proposed converter are presented in Figure 8. The converter does not require the incorporation of any additional cooling system owing to the design parameters. Herein, many flyback converters may be connected serially to obtain DC bus for the establishment of telecommunication systems.

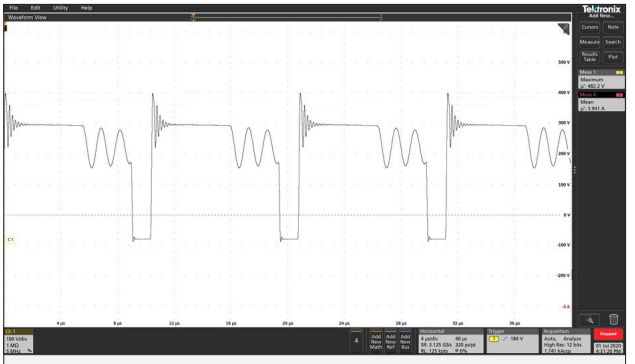

**Figure 6.** The voltage stresses of the MOSFET for 265 V RMS

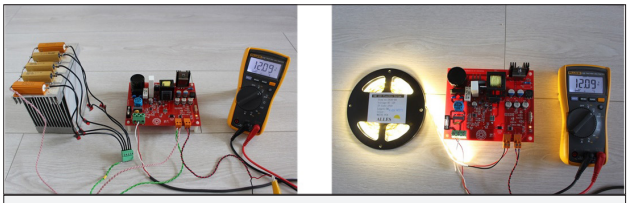

**Figure 7.** The image of the prototype of the proposed flyback converter for a) resistive load and b) LED load.

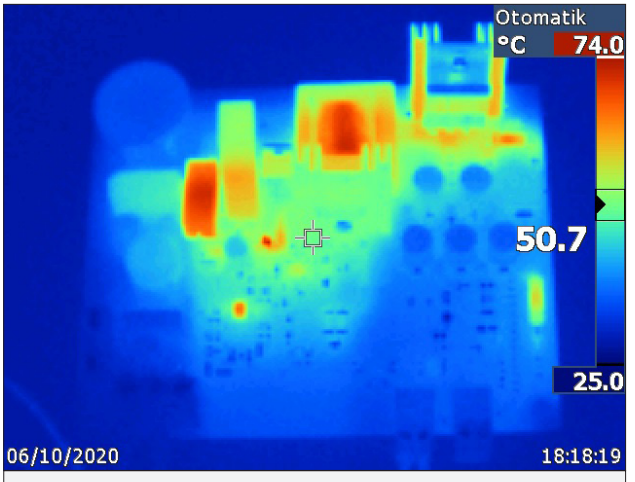


**Figure 8.** The thermal image of the prototype of the proposed flyback converter

**Table 3.** The experimental results for different input voltages under various load stages

| **AC Input Voltage** | | | | | | |
|---|---|---|---|---|---|---|
| **$V_i$ =85 V** | | | | | | |
| **Load Condition** | **$V_i$ (V)** | **$I_i$ (A)** | **$P_i$ (W)** | **$V_o$ (V)** | **$I_o$ (A)** | **Efficiency (%)** |
| Stage 1 (~%20) | 86.49 | 0.339 | 12.75 | 12.02 | 0.8 | 77.77255 |
| Stage 2 (~%40) | 85.82 | 0.528 | 24.31 | 12.02 | 1.6 | 80.34554 |
| Stage 3 (~%60) | 85.88 | 0.748 | 36.06 | 12.01 | 2.4 | 80.76539 |
| Stage 4 (~%80) | 86.3 | 0.984 | 47.83 | 12.02 | 3.2 | 81.04537 |
| Stage 5 (~%100) | 85.98 | 1.237 | 60.17 | 12.02 | 4 | 80.40552 |
| **AC Input Voltage** | | | | | | |
| **$V_i$ =220 V** | | | | | | |
| **Load Condition** | **$V_i$ (V)** | **$I_i$ (A)** | **$P_i$ (W)** | **$V_o$ (V)** | **$I_o$ (A)** | **Efficiency (%)** |
| Stage 1 (~%20) | 222.3 | 0.252 | 14.11 | 12.14 | 0.8 | 70.95677 |
| Stage 2 (~%40) | 221.7 | 0.343 | 26.18 | 12.11 | 1.6 | 75.15661 |
| Stage 3 (~%60) | 222.4 | 0.418 | 37.1 | 12.09 | 2.4 | 79.01887 |
| Stage 4 (~%80) | 222 | 0.5 | 48.1 | 12.08 | 3.2 | 80.9896 |
| Stage 5 (~%100) | 222.6 | 0.582 | 60.09 | 12.08 | 4 | 80.91197 |
| **AC Input Voltage** | | | | | | |
| **$V_i$ =265 V** | | | | | | |
| **Load Condition** | **$V_i$ (V)** | **$I_i$ (A)** | **$P_i$ (W)** | **$V_o$ (V)** | **$I_o$ (A)** | **Efficiency (%)** |
| Stage 1 (~%20) | 264.6 | 0.155 | 15.47 | 12.01 | 0.8 | 64.04654 |
| Stage 2 (~%40) | 263.9 | 0.248 | 26.69 | 12.01 | 1.6 | 73.12102 |
| Stage 3 (~%60) | 264.6 | 0.333 | 37.83 | 12.02 | 2.4 | 77.04996 |
| Stage 4 (~%80) | 264 | 0.418 | 49.19 | 12.01 | 3.2 | 78.73958 |
| Stage 5 (~%100) | 265.2 | 0.497 | 60.96 | 12.01 | 4 | 79.2979 |

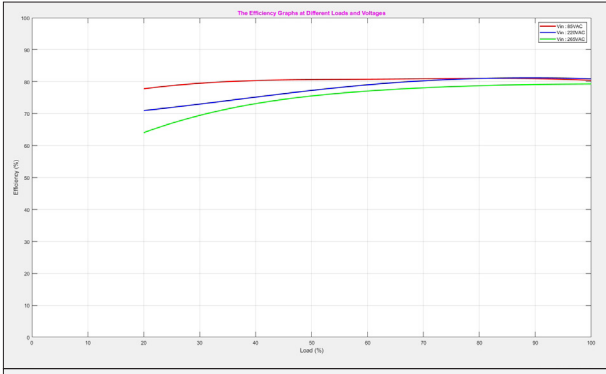


**Figure 9.** The efficiency curve for the universal input voltages with wide load ranges

The efficiency values are provided for different input voltages and load stages in Table 3.

Thus, the efficiency curves according to universal input voltage range with wide load ranges are presented in Figure 9. It can be inferred that higher efficiency than 80% is achieved, which is obtained using the design procedure.

**Discussion**

In this study, we have presented a flyback converter which can be operated under universal input voltage with wide load ranges. The detailed theoretical analysis is conducted and verified using an implementation of DCM flyback converter for 85 V-265 V RMS AC input voltage, 12 $V_o$ output voltage, 100

kHz switching frequency, and 48 W output power. The voltage stresses of the MOSFET cannot exceed 400 V at the worst conditions. The overall efficiency of the proposed converter at full load was determined to be 81% for the universal input. The thermal measurements were provided for the proposed flyback converter. No external cooling systems were necessary, and this resulted in a small-volume design with ease of application in industrial systems that require the inclusion of more serial flyback converters.

**Peer-review:** Externally peer-reviewed.

**Author Contributions:** Concept – F.G., E.A., A.H.O.; Design – F.G., E.A., A.H.O.; Supervision – F.G., E.A., A.H.O.; Resources – F.G., E.A., A.H.O.; Materials – F.G., E.A., A.H.O.; Data Collection and/or Processing – F.G., E.A., A.H.O.; Analysis and/or Interpretation – F.G., E.A., A.H.O.; Literature Search – F.G., E.A., A.H.O.; Writing Manuscript – F.G., E.A., A.H.O.; Critical Review – F.G., E.A., A.H.O.

**Conflict of Interest:** The authors have no conflicts of interest to declare.

**Financial Disclosure:** The authors declared that this study has received no financial support.

## References

1. Y. Wang, J. M. Alonso, X. Ruan, "A review of LED drivers and related technologies," IEEE Trans Industrial Electron., vol. 64, no.7, pp. 5754-5765, March, 2017. [Crossref]
2. M. O. Badawy, Y. Sozer, J. A. "De Abreu-Garcia, A novel control for a cascaded buck-boost PFC converter operating in discontinuous capacitor voltage mode," IEEE Trans. Ind. Electron., vol. 63, no. 7, pp. 4198-4200, March, 2016. [Crossref]
3. H. Bodur, H. Yesilyurt, E. Akboy, "Passive lossless snubber for PFC ac-dc converters," Electrica, vol. 20, no.1, pp. 98-107, Jan., 2020. [Crossref]
4. B. Akin, "Snubber circuit application for power factor correction flyback led driver," Electrica, vol. 20, no.1, pp. 108-116, Jan., 2020.
5. H. J. Chiu, Y. K. Lo, J. T Chen, S. J. Cheng, C. Y. Lin, S. C. Mou, "A high-efficiency dimmable LED driver for low-power lighting applications," IEEE Trans. Ind. Electron., vol.57, no.2, pp. 735-743, March, 2010. [Crossref]
6. C. B. Park, B. H. Choi, J. P. Cheon, C. T. Rim, "Robust active LED driver with high power factor and low total harmonic distortion compatible with a rapid-start ballast," J Power Electron, vol.14, no.2, pp. 226-36, Jan, 2014. [Crossref]
7. B. Poorali, E. Adib, H. Farzanehfard, "A Single-Stage Single-Switch Soft-Switching Power-Factor-Correction LED Driver," IEEE Trans. Power Electron., vol.32, no.10, pp. 7932-40, Dec., 2017. [Crossref]
8. N. Weidong, Y. Zongguang, W. Haibing, G. Bin, T. Long, Y. Lihang, "A PSR single-stage flyback LED driver with simple line regulation and quasi-resonant operation," J of Semiconductors, vol.35, no.8, pp. 1-6, Jan., 2014. [Crossref]
9. C. A. Cheng, H.L. Cheng, F.L. Yang, C.W. Ku, "Single-stage driver for supplying high-power light-emitting-diodes with universal utility-line input voltages," IET Power Electron., vol.5, no.9, pp. 1614-1623, Nov., 2011. [Crossref]
10. T. Zhan, Y. Zhang, J. Nie, Y. Zhang, Z. Zhao, "A novel soft-switching boost converter with magnetically coupled resonant snubber," IEEE Trans. Power Electron., vol.29, no.11, 5680-5687, Jan., 2014. [Crossref]
11. Y. Şahin, N.S. Ting, "Soft switching passive snubber cell for family of PWM DC-DC converters," Electrical Enginnering, vol.100, pp. 1785-1796, Apr., 2018. [Crossref]
12. M. Mohammadi, E. Adib, M. R. Yazdani, "Family of soft-switching single-switch PWM converters with lossless passive snubber," IEEE Trans. Ind. Electron.,vol.62, no.6, pp. 3473-3481, Nov., 2015.
13. N. Kondrath, M. K. Kazimierczuk, "Comparison of wide- and highfrequency duty-ratio-to-inductor-current transfer functions of DC-DC PWM buck converter in CCM," IEEE Trans. Ind. Electron.,vol.59, no.1, pp. 641-642, March, 2012. [Crossref]
14. Y. Wang, Y. Guan, K. Ren, W. Wang, D. Xu, "A single-stage LED driver based on BCM boost circuit and LLC converter for street lighting system," IEEE Trans. Ind. Electron., vol.62, no.9, pp. 5446-5448, March, 2015. [Crossref]
15. R.T.H. Li, H.S H. Chung, A.K.T. Sung, "Passive lossless snubber for boost PFC with minimum voltage and current stress," IEEE Trans. Power Electron., vol.25, no.3, pp. 602-613, Oct., 2010. [Crossref]

Ferudun Gökcegöz was born in Istanbul, Turkey, in 1987. He received a B.S. degree in electrical-electronics engineering from Sakarya University (SAU), Sakarya, Turkey, in 2010, and an M.S. degree in electrical engineering from Yildiz Technical University (YTU), Istanbul, Turkey, in 2019. He is currently pursuing his Ph.D. education at the Yildiz Technical University. He was an Embedded Systems R&D Engineer at Sisel Engineering (Enda) in 2010-2014, at Grup Arge in 2015-2017, and at Elartek Engineering in 2017-2019, respectively. He has worked as an R&D Engineer at Power Elektronik A.S since 2019. He has worked on various embedded systems projects, Iot-based remote control projects, and power electronics projects. His current research and work interests include DC-DC converters, switch mode power supplies, embedded software, and hardware systems.

Erdem Akboy was born in Istanbul, Turkey, in 1987. He received a B.S. degree in electrical-electronics engineering from Sakarya University, Sakarya, Turkey, in 2009, and M.S. and Ph.D. degrees in electrical engineering from Yildiz Technical University, Esenler, Turkey, in 2012 and 2018, respectively, where he is currently working as a research assistant. His current research interests include soft switching, grid connected converter, power factor correction (PFC), inverters, energy storage systems, and DC-DC converters.

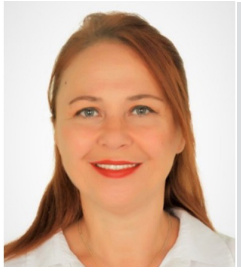

Atiye Hulya Obdan was born in İstanbul, Turkey, in 1967. She received her B.S degree in 1989, M.Sc. degree in 1993, and Ph.D degree in 2002, in Electrical Engineering from Yildiz Technical University. She is currently working as an Associate Professor in Electrical Engineering Department of Yildiz Technical University, Istanbul, Turkey. Her research interests include the control of electrical machinery, control design in power electronics circuits and their applications, switching power supplies, resonant converters, and converter topologies for renewable energy applications.